

currents of  $<20 \text{ cm s}^{-1}$ , as observed during SERIES. Trapping efficiency is thought to be determined by the characteristics of sinking particles, trap design and upper-ocean hydrodynamics<sup>19</sup>. The location of the 'In' traps relative to the patch was monitored using a logging fluorometer 10 m subsurface on the surface-tethered array. Traps remained near the patch centre; on day 23 the array was at the periphery for 36 h before recovery and therefore underestimated vertical export. 'Out' traps were deployed at least 20 km northeast of the patch. Limited replicates were available from trap cups, and the standard error ( $n = 3$ ) for fluxes was  $\pm 1.3 \text{ mmol Si m}^{-2} \text{ d}^{-1}$  and  $\pm 2.5 \text{ mmol C m}^{-2} \text{ d}^{-1}$  for the 75 and 100 m 'In' traps on day 14.

**Bacterial remineralization of particles**

We had no information on bacterial growth efficiency, which was required to calculate bacterial carbon demand<sup>20</sup>: demand = bacterial production  $\times$  (1/growth efficiency), published values display a range from 0.1 to 0.7 (ref. 29). Therefore, we employed indirect approaches (changes in DIC concentrations, selective preservation of opal and ammonium accumulation) to estimate particle remineralization.

Received 16 November 2003; accepted 24 February 2004; doi:10.1038/nature02437.  
Published online 17 March 2004.

1. Coale, K. H. *et al.* A massive phytoplankton bloom induced by an ecosystem-scale iron fertilization experiment in the equatorial Pacific Ocean. *Nature* **383**, 495–501 (1996).
2. Boyd, P. W. *et al.* A mesoscale phytoplankton bloom in the polar Southern Ocean stimulated by iron fertilization. *Nature* **407**, 695–702 (2000).
3. Buesseler, K. O. & Boyd, P. W. Will ocean fertilization work? *Science* **300**, 67–68 (2003).
4. Gervais, F., Riebesell, U. & Gorbunov, M. Y. Changes in primary productivity and chlorophyll *a* in response to iron fertilization in the Southern Polar Frontal Zone. *Limnol. Oceanogr.* **47**, 1324–1335 (2002).
5. Tsuda, A. *et al.* A mesoscale iron enrichment in the western Subarctic Pacific induces a large centric diatom bloom. *Science* **300**, 958–961 (2003).
6. Martin, J. H. Glacial-interglacial CO<sub>2</sub> change: The iron hypothesis. *Paleoceanography* **5**, 1–13 (1990).
7. Matsumoto, K., Sarmiento, J. L. & Brzezinski, M. A. Silicic acid leakage from the Southern Ocean: A possible explanation for glacial atmospheric pCO<sub>2</sub>. *Glob. Biogeochem. Cycles* **16**, doi:10.1029/2001GB001442 (2002).
8. Chisholm, S. W., Falkowski, P. G. & Cullen, J. J. Oceans—Discrediting ocean fertilization. *Science* **294**, 309–310 (2001).
9. Petit, J. R. *et al.* Climate and atmospheric history of the past 420,000 years from the Vostok ice core, Antarctica. *Nature* **399**, 429–436 (1999).
10. Tabata, S. The general circulation of the Pacific Ocean and a brief account of the oceanographic structure of the North Pacific Ocean. Part I—Circulation and volume transports. *Atmosphere* **13**, 133–168 (1975).
11. Nishioka, J., Takeda, S., Wong, C. S. & Johnson, W. K. Size-fractionated iron concentrations in the northeast Pacific Ocean: distribution of soluble and small colloidal iron. *Mar. Chem.* **74**, 157–179 (2001).
12. LaRoche, J., Boyd, P. W., McKay, R. M. L. & Geider, R. J. Flavodoxin as an *in situ* marker for iron stress in phytoplankton. *Nature* **382**, 802–805 (1996).
13. Cullen, J. J. Hypothesis to explain high-nutrient conditions in the open sea. *Limnol. Oceanogr.* **36**, 1578–1599 (1991).
14. Strathmann, R. R. Estimating the organic carbon content of phytoplankton from cell volume or plasma volume. *Limnol. Oceanogr.* **12**, 411–418 (1967).
15. Komar, P. D., Morse, A. P., Small, L. F. & Fowler, S. W. An analysis of sinking rates of natural copepod and euphausiid fecal pellets. *Limnol. Oceanogr.* **26**, 172–180 (1981).
16. Bidle, K. D., Manganello, M. & Azam, F. Regulation of oceanic silicon and carbon preservation by temperature control on bacteria. *Science* **298**, 1980–1984 (2002).
17. Smith, D. C., Simon, M., Alldredge, A. L. & Azam, F. Intense hydrolytic enzyme activity on marine aggregates and implications for rapid particle dissolution. *Nature* **359**, 139–142 (1992).
18. Dagg, M. Sinking particles as a possible source of nutrition for the large calanoid copepod *Neocalanus cristatus* in the sub-arctic Pacific Ocean. *Deep-Sea Res.* **1** **40**, 1431–1445 (1993).
19. Buesseler, K. O., Michaels, A. F., Siegel, D. A. & Knap, A. H. A 3-dimensional time-dependent approach to calibrating sediment trap fluxes. *Glob. Biogeochem. Cycles* **8**, 179–193 (1994).
20. Treguer, P. *et al.* The silica balance in the world ocean: a re-estimate. *Science* **268**, 375–379 (1995).
21. Sunda, W. G. & Huntsman, S. A. Iron uptake and growth limitation in oceanic and coastal phytoplankton. *Mar. Chem.* **50**, 189–206 (1995).
22. Buesseler, K. O. The decoupling of production and particulate export in the surface ocean. *Glob. Biogeochem. Cycles* **12**, 297–310 (1998).
23. Harrison, K. G. Role of increased marine silica input on paleo-pCO<sub>2</sub> levels. *Paleoceanography* **15**, 292–298 (2000).
24. Law, C. S., Abraham, E. R., Watson, A. J. & Liddicoat, M. Vertical diffusion and nutrient supply to the surface mixed layer of the Antarctic Circumpolar Current. *J. Geophys. Res.* **108**, doi:10.1029/2002JC001604 (2003).
25. Abraham, E. R. *et al.* Importance of stirring in the development of an iron-fertilized phytoplankton bloom. *Nature* **407**, 727–730 (2000).
26. Honda, M. C. *et al.* The biological pump in the northwestern North Pacific based on fluxes and major components of particulate matter obtained by sediment-trap experiments (1997–2000). *Deep-Sea Res.* **II** **49**, 5595–5625 (2002).
27. Bishop, J. K. B. Transmissometer measurement of POC. *Deep-Sea Res.* **1** **46**, 353–369 (1999).
28. Tsuda, A. & Sugisaki, H. In-situ grazing rate of the copepod population in the western subarctic North Pacific during spring. *Mar. Biol.* **120**, 203–210 (1994).
29. Rivkin, R. & Legendre, L. Biogenic carbon cycling in the upper ocean: effects of microbial respiration. *Science* **291**, 2398–2400 (2001).
30. Siegel, D. A., Granata, T. C., Michaels, A. F. & Dickey, T. D. Mesoscale eddy diffusion, particle sinking, and the interpretation of sediment trap data. *J. Geophys. Res.* **95**, 5305–5311 (1990).

Supplementary Information accompanies the paper on [www.nature.com/nature](http://www.nature.com/nature).

**Acknowledgements** We thank the officers and crews and scientists on board the *John P. Tully*, *El Puma* and *Kaiyo Maru*. We are grateful to S. Toews for shoreside logistical support. The manuscript was improved by comments from K. Currie, R. Frew, C. Hurd, P. Boyd, D. Hutchins and T. Trull. This study was supported by NSERC Canada as part of the C-SOLAS programme, CFCAS, DFO PERD (Canada), the New Zealand PGSF (Ocean Ecosystems), and the Global Environmental Research Fund from the Ministry of Environment, the Fisheries Agency, and the Central Research Institute of Electric Power Industry research funding (Japan).

**Competing interests statement** The authors declare that they have no competing financial interests.

**Correspondence** and requests for materials should be addressed to P.W.B. ([p.boyd@niwa.co.nz](mailto:p.boyd@niwa.co.nz)).

.....  
**Ferns diversified in the shadow of angiosperms**

**Harald Schneider<sup>1,2</sup>, Eric Schuettpelz<sup>1</sup>, Kathleen M. Pryer<sup>1</sup>, Raymond Cranfill<sup>3</sup>, Susana Magallón<sup>4</sup> & Richard Lupia<sup>5,6</sup>**

<sup>1</sup>*Department of Biology, Duke University, Durham, North Carolina 27708, USA*  
<sup>2</sup>*Albrecht-von-Haller-Institut für Pflanzenwissenschaften, Abteilung Systematische Botanik, Georg-August-Universität, Untere Karspüle 2, 37073 Göttingen, Germany*  
<sup>3</sup>*University Herbarium, University of California, 1001 Valley Life Sciences Building #2465, Berkeley, California 94720, USA*  
<sup>4</sup>*Departamento de Botánica, Instituto de Biología, Universidad Nacional Autónoma de México, Circuito Exterior, Anexo al Jardín Botánico, AP 70-233, México DF 04510, Mexico*  
<sup>5</sup>*Sam Noble Oklahoma Museum of Natural History and*  
<sup>6</sup>*School of Geology and Geophysics, University of Oklahoma, Norman, Oklahoma 73072, USA*

The rise of angiosperms during the Cretaceous period is often portrayed as coincident with a dramatic drop in the diversity and abundance of many seed-free vascular plant lineages, including ferns<sup>1–5</sup>. This has led to the widespread belief that ferns, once a principal component of terrestrial ecosystems<sup>6</sup>, succumbed to the ecological predominance of angiosperms and are mostly evolutionary holdovers from the late Palaeozoic/early Mesozoic era. The first appearance of many modern fern genera in the early Tertiary fossil record implies another evolutionary scenario; that is, that the majority of living ferns resulted from a more recent diversification<sup>7–10</sup>. But a full understanding of trends in fern diversification and evolution using only palaeobotanical evidence is hindered by the poor taxonomic resolution of the fern fossil record in the Cretaceous<sup>11</sup>. Here we report divergence time estimates for ferns and angiosperms based on molecular data, with constraints from a reassessment of the fossil record. We show that polypod ferns (>80% of living fern species) diversified in the Cretaceous, after angiosperms, suggesting perhaps an ecological opportunistic response to the diversification of angiosperms, as angiosperms came to dominate terrestrial ecosystems.

The extraordinary diversification of angiosperms throughout the Cretaceous and Tertiary, culminating in an estimated 250,000–300,000 living species<sup>3</sup>, is well known<sup>1–4,12</sup> owing to the exceptional fossil record of this lineage. The oldest fossils (Early Cretaceous) that can be unequivocally assigned to specific clades of angiosperms<sup>3,12,13</sup> correspond to the initially diverging lineages resolved in DNA-based phylogenetic analyses<sup>14–16</sup>. The well-sampled fossil record of subsequently derived angiosperms is also broadly congruent with phylogenetic analyses<sup>12,14–16</sup>. Ferns, with more than 10,000 living species, are the second largest group of vascular plants<sup>7</sup>. They attained remarkable levels of diversity and abundance from the Carboniferous to the Jurassic—a richness that is well

documented in the geologic record<sup>9,10,17</sup>—but these levels were shown to have sharply declined in the Cretaceous<sup>4,5</sup>. This observation of a decline has been directly attributed to the concurrent rise to dominance by angiosperms<sup>1</sup>.

Within ferns, strong support has been demonstrated for the monophyly of polypods, a hyperdiverse derived lineage<sup>18</sup> to which the vast majority of Tertiary fern fossils belong. Whereas the virtual absence of unambiguous polypod fossils in the Cretaceous favours a Tertiary radiation, startling new discoveries from the Early Cretaceous of well-preserved polypod sporangia<sup>19</sup> (Neocomian) and roots<sup>11</sup> (Albian) seem to imply that the divergence of polypods had begun by the start of the Cretaceous. We aimed to determine which of these two hypotheses—Tertiary versus Cretaceous radiation of polypods—is best supported, on the basis of an independent analysis of DNA sequence data with integrated fossil time constraints.

We obtained DNA sequence data from two chloroplast genes (*rbcL*, *rps4*) for 45 polypods and other fern taxa to reconstruct phylogenetic relationships using bayesian methods. We used the resulting phylogenetic consensus to re-evaluate critical fern fossils (Supplementary Information) and assign them to extant lineages based on morphological synapomorphies. Using these fossils as age constraints, we estimated divergence times with penalized likelihood<sup>20</sup> across the fern consensus phylogeny. To evaluate the effects of phylogenetic uncertainty<sup>21</sup> due to both topological and branch-length estimation error we also estimated divergence times across 1,000 randomly sampled bayesian trees. To allow for consideration of the fern results relative to angiosperms, we assembled a three-gene (chloroplast *rbcL* and *atpB*, and nuclear small-subunit ribosomal DNA) data set consisting of 95 taxa, reconstructed angiosperm relationships, and estimated their divergence times across the angiosperm consensus phylogeny and 1,000 randomly sampled bayesian trees. For angiosperms, we applied fossil age constraints<sup>22</sup> (Table 1) in two ways, differing only in the application of the fossil age of the angiosperm crown group. We were either strict (fixed the age at 132 Myr; ref. 22) or relaxed (applied 132 Myr as a minimum age constraint) in our application of this fossil age. Our phylogenetic results for ferns and angiosperms, plotted against the geological timescale, are shown in Fig. 1. Age estimates, means and standard deviations for well-supported nodes (posterior probability  $\geq 0.95$ ) are provided in Table 1.

Our phylogenetic analyses of ferns (Fig. 1a) largely confirm relationships observed in prior studies<sup>18</sup>, with osmundaceous ferns (*Osmunda*) resolved as the earliest-diverging leptosporangiate lineage followed, in order of divergence, by filmy ferns (*Hymenophyllum*), gleichenioids (*Gleichenia*), schizaeoids (*Lygodium*), water ferns (*Marsilea* + *Salvinia*), tree ferns (*Plagiogyria* to *Dicksonia*) and polypods. Basal within the polypods is a grade of enigmatic genera (*Lonchitis* and *Saccoloma*) and species-poor families leading to a large clade of derived ferns that is composed of two major, species-rich clades—pteridoids and eupolypods. These two clades include 80% of all living fern species. Eupolypods, which comprise 67% of living ferns, consist of two subclades, eupolypods I and eupolypods II. Our divergence time estimates for ferns are mostly older than those implied by the fossil record but show small standard deviations (Table 1). We find that polypod ferns (node a10), derived ferns (node a15) and eupolypods (node a21) began to diversify during the Middle Jurassic, Late Jurassic, and Albian (Early Cretaceous), respectively (Fig. 1a). The major lineages of derived ferns—pteridoids, eupolypods I and eupolypods II (nodes a16, a22 and a25, respectively)—diversified in the Late Cretaceous.

The results of our phylogenetic analyses of angiosperms (Fig. 1b) mostly agree with previously proposed relationships<sup>14</sup>. The minor discrepancies between our phylogeny and other published trees are mostly due to taxonomic sampling differences and do not affect our divergence time estimates for angiosperms. Depending on how we

treated the fossil age of the angiosperm crown group (132 Myr; ref. 22), our divergence time estimates for angiosperms varied. If we were strict in our application of this fossil age (that is, fixed the age of node b10) our age estimates were mostly consistent with the fossil record (Fig. 1b, black tree), with the major lineages of angiosperms, such as euasterids I, euasterids II, eurosids II, and core monocots (nodes b46, b40, b55, and b18, respectively) radiating in the Late Cretaceous. If we were relaxed in our application (that is, applied a minimum age constraint to node b10) our age estimates were more in line with those of previous molecular-based studies<sup>23</sup> (Fig. 1b, grey tree), with the major lineages of angiosperms radiating in the Middle Jurassic to Early Cretaceous.

Lineages-through-time plots based on the chronograms presented in Fig. 1a and b document the accumulation of polypod and angiosperm lineages, primarily in the Mesozoic (Fig. 1c). The initiation of the major diversification of polypods, which we estimate at approximately 100 Myr, took place subsequent to the radiation of angiosperms, regardless of whether we fixed the age of the angiosperm crown group, or merely applied a minimum age constraint to this node (Fig. 1c). To the best of our knowledge, this relationship between polypod and angiosperm diversification—polypods evolving in the ‘shadow of angiosperms’—has never before been demonstrated, although it has been suggested<sup>1,7–9</sup>.

Our present finding of a Cretaceous increase in polypod diversity, based on divergence time estimates, was not recovered in previous investigations of the diversity and abundance of land plants through the Cretaceous and Early Tertiary<sup>2,4,5</sup>. Most of these other studies, using macrofossil and palynological data, essentially proposed a replacement of seed-free vascular plants by angiosperms, and did not consider specifically the more restricted group of polypods. Recovering an increase in polypod diversity through the Cretaceous, as we did here, is not possible when relying only on the currently available fossil record because of such inherent biases as: (1) the vast majority of palaeobotanical studies have focused on angiosperms rather than ferns; (2) many polypods are epiphytes or occupy other ecological niches that are less likely to be preserved; and perhaps most importantly (3) unlike their living counterparts, fossilized polypod spores are usually plain and unsculptured due to perine detachment, which erases their species diversity in the fossil record. An exclusively molecular approach, however, also has its limitations<sup>24</sup>. Integrating fossil time constraints together with molecular data is an increasingly powerful tool for identifying historical trends and events across the tree of life<sup>25</sup>.

Although the proliferation of angiosperms in the Cretaceous is indeed coupled with the decline of many seed-free vascular plant lineages, their radiation also created new ecospace into which certain lineages could diversify. Such an ecological opportunistic response to the spatially more diverse and complex habitats provided by angiosperms, compared to gymnosperms, has been proposed for epiphytic homosporous lycophytes (Lycopodiaceae) using methods related to those used here<sup>26</sup>, and may also apply to the Cretaceous radiation of polypod ferns. Many modern-day polypods preferentially grow under the low-light canopy conditions present in angiosperm forests. An unconventional photoreceptor, phytochrome 3 (*PHY3*)<sup>27,28</sup>, recently identified in the polypod fern *Adiantum*, may provide an ecophysiological explanation for much polypod diversification in these shady habitats. *PHY3* is a chimaeric protein with a red/far-red light receptor phytochrome at its amino-terminal end and a blue-light absorbing phototropin at its carboxy-terminal end. Although the light-induced signalling mechanism of *PHY3* is yet to be solved, its capacity to couple the photosensitivity of phytochrome with phototropin kinase activity would allow both red and blue light to function in phototropism and chloroplast movement, thereby conferring a distinct advantage under low-light canopy conditions<sup>27</sup>. *PHY3* appears to be restricted to polypod ferns and has not been found in any of the basal fern lineages or seed plants<sup>27</sup>.

The rise of angiosperms undoubtedly initiated fundamental changes in terrestrial ecosystems and set in motion processes that had important consequences for most extant terrestrial biodiversity. Yet, because of ambiguity regarding the timing of angiosperm forest establishment<sup>1</sup>, it is not possible for us to confirm that polypods diversified within the dense forest ecospaces created by angiosperms or that the chimaeric photoreceptor *PHY3* was a critical innovation necessary for the radiation of polypods. The diversification that we

observe in polypods may be a response to an abiotic stimulus (for example, a decline in CO<sub>2</sub>; climate change, such as global warming; increased tectonic activity or other major geological events). Nevertheless, the results of our study point toward the time period to focus on, to test causal hypotheses concerning the radiation of polypods. Potential links between profound biological events, such as the establishment of angiosperm forests and the diversification of polypods, or between these events and large-scale extrinsic factors,

Table 1 Fossil age constraints and molecular age estimates

Node*	Lineage	Fossil age (Myr)†	Molecular age (Myr)		Node*	Lineage	Fossil age (Myr)†	Molecular age (Myr)		Relaxed molecular age (Myr)	
			Estimate‡	Mean ± s.d.§				Estimate‡	Mean ± s.d.§	Estimate‡	Mean ± s.d.§
a01	Euphyllophytes	380.00	380.00	380.00 ± 0.00	b01	Euphyllophytes	380.00	380.00	380.00 ± 0.00	380.00	380.00 ± 0.00
a02	Seed plants	310.00	310.00	310.00 ± 0.00	b02	Monilophytes	354.00	354.00	354.00 ± 0.00	354.00	354.00 ± 0.00
a03	Monilophytes	354.00	354.00	354.00 ± 0.00	b03	Seed plants	329.38	329.38	328.96 ± 2.80	334.18	333.10 ± 3.52
a04	Leptosporangiates	280.00	307.08	307.90 ± 8.65	b04		320.19	320.19	320.18 ± 1.90	322.57	322.23 ± 2.43
a05		270.00	281.84	283.47 ± 8.99	b05		310.00	310.00	310.00 ± 0.00	310.00	310.00 ± 0.00
a06			218.04	222.99 ± 9.12	b06	Gnetales		184.82	184.71 ± 8.56	184.91	188.94 ± 11.54
a07	Water ferns	137.00	157.98	161.59 ± 13.60	b07			135.63	136.31 ± 9.00	135.72	140.77 ± 11.90
a08	Tree ferns		188.34	191.94 ± 11.18	b08	Conifers		265.47	266.50 ± 11.80	265.52	263.75 ± 12.99
a09		159.00	159.00	159.42 ± 2.66	b09			210.99	212.36 ± 13.33	211.06	209.66 ± 14.16
a10	Polypods	121.00	175.75	181.87 ± 9.48	b10	angiosperms	132.00	132.00	132.00 ± 0.00	251.77	246.36 ± 14.91¶
a11		99.00	159.28	165.34 ± 9.47	b11			130.37	130.32 ± 0.54	232.12	226.27 ± 15.45¶
a12	Lindsaeoids		97.53	103.47 ± 9.75	b12	Nymphaeaceae	121.00	121.00	121.00 ± 0.00	121.00	121.00 ± 0.00
a13			151.42	155.43 ± 9.65	b13			130.78	130.79 ± 0.34	243.22	237.65 ± 15.60¶
a14	Dennstaedtioids		113.93	118.34 ± 12.59	b14	Austrobaileyales		85.12	85.37 ± 6.84	168.02	158.31 ± 27.13¶
a15	Derived ferns	93.50	144.53	148.56 ± 9.44	b15			129.49	129.50 ± 0.42	234.50	229.11 ± 15.61¶
a16	Pteridooids		97.41	100.75 ± 6.72	b16	Monocots		116.47	116.48 ± 2.36	207.08	204.05 ± 13.12¶
a17		37.00	80.22	83.40 ± 6.18	b17		99.00	107.51	107.49 ± 2.63	189.89	187.70 ± 11.34¶
a18			73.93	76.92 ± 6.29	b18	Core monocots		97.39	97.29 ± 3.15	171.09	169.56 ± 10.28
a19		65.00	80.50	83.34 ± 6.32	b19	Commelinids		86.66	87.56 ± 3.57	152.82	153.16 ± 10.10
a20			57.08	59.17 ± 5.23	b20			81.18	82.02 ± 3.58	142.86	143.37 ± 9.72
a21	Eupolypods		104.69	107.29 ± 8.36	b21	Poales	65.00	70.52	71.25 ± 3.65	123.38	124.15 ± 9.11
a22	Eupolypods I		93.61	96.70 ± 7.96	b22	Laurales	105.50	105.50	105.55 ± 0.42	165.94	159.65 ± 21.62
a23			72.73	75.10 ± 6.97	b23	Piperales		108.05	109.24 ± 3.43	186.32	182.55 ± 16.18¶
a24			47.67	49.57 ± 4.84	b24	Aristolochiaceae	89.00	90.70	92.30 ± 3.71	157.39	153.31 ± 16.33¶
a25	Eupolypods II		94.52	95.55 ± 8.59	b25			69.01	69.69 ± 4.44	117.29	115.38 ± 11.36
a26			55.50	55.22 ± 5.69	b26	Canellales	121.00	121.00	121.00 ± 0.00	157.06	149.65 ± 17.37
a27			40.44	40.21 ± 4.55	b27	Magnoliales	96.00	101.93	102.62 ± 5.21	158.15	152.81 ± 18.47¶
a28			63.64	70.45 ± 9.38	b28	Chloranthaceae	121.00	121.00	121.00 ± 0.00	124.31	128.77 ± 10.56
a29		65.00	69.70	74.13 ± 7.84	b29			128.22	128.06 ± 0.71	229.35	222.92 ± 15.87¶
a30		37.00	54.88	58.17 ± 6.99	b30	Eudicots	121.00	123.31	123.17 ± 0.92	209.59	203.49 ± 16.14¶
					b31		99.00	120.19	120.62 ± 1.06	196.49	193.41 ± 15.60¶
					b32	Core eudicots		116.25	116.68 ± 1.10	180.31	178.97 ± 13.60¶
					b33		49.00	100.41	101.44 ± 4.61	154.14	154.14 ± 13.81¶
					b34	Santalales	49.00	87.41	87.58 ± 4.12	131.31	131.68 ± 10.34
					b35	Caryophyllales	83.50	83.50	84.76 ± 2.23	121.75	123.42 ± 9.59
					b36	Asterids	103.50	104.97 ± 1.88	104.97 ± 1.88	151.06	154.58 ± 12.03¶
					b37	Cornales	85.80	85.80	85.98 ± 0.79	117.42	116.78 ± 17.12
					b38	Ericales	89.00	89.00	89.15 ± 0.75	120.41	122.94 ± 11.28
					b39			97.22	99.27 ± 2.36	141.26	146.06 ± 11.29¶
					b40	Euasterids II		87.98	90.02 ± 3.38	129.54	133.27 ± 12.33¶
					b41			83.61	85.57 ± 3.60	123.64	126.97 ± 12.38¶
					b42			76.96	78.75 ± 3.94	113.31	116.47 ± 11.32
					b43			75.54	78.01 ± 4.63	115.18	116.66 ± 16.08¶
					b44			69.40	71.52 ± 4.79	106.57	107.45 ± 15.79¶
					b45	Apiales	37.00	50.91	52.40 ± 5.02	80.13	80.19 ± 14.38¶
					b46	Euasterids I		91.90	93.81 ± 2.78	132.75	137.63 ± 10.19¶
					b47			78.26	79.85 ± 2.93	111.45	116.38 ± 7.65
					b48	Solanales	33.70	67.56	68.69 ± 3.61	95.88	99.93 ± 7.21
					b49	Lamiales	33.70	53.38	54.92 ± 3.91	75.78	80.15 ± 7.07
					b50	Gentianales	33.70	58.44	59.84 ± 3.62	82.40	86.81 ± 6.45
					b51			114.68	115.13 ± 1.20	173.54	172.53 ± 12.85¶
					b52	Saxifragales	89.00	89.00	89.01 ± 0.30	112.78	108.73 ± 15.01
					b53	Rosids		110.28	110.80 ± 1.29	156.83	157.13 ± 10.17¶
					b54	Myrtales	85.80	85.80	85.81 ± 0.21	104.36	106.07 ± 8.88
					b55	Eurosid II		97.09	97.96 ± 2.71	133.01	133.71 ± 9.09
					b56	Sapindales	65.00	65.00	65.15 ± 0.69	82.12	80.49 ± 7.82
					b57	Malvales	68.00	71.83	72.92 ± 3.65	97.64	98.53 ± 7.38
					b58	Brassicales		55.27	57.86 ± 5.59	76.87	79.92 ± 10.25
					b59	"Eurosid I"		104.49	104.38 ± 1.34	137.92	137.02 ± 7.47
					b60	Fabales		91.60	90.67 ± 4.09	120.61	118.90 ± 7.96
					b61	Fagales	93.50	93.50	93.50 ± 0.00	93.50	93.53 ± 0.38
					b62	Cucurbitales	54.80	77.01	77.25 ± 4.48	99.74	100.54 ± 7.38
					b63	Rosales	65.00	86.69	86.93 ± 4.47	112.76	113.52 ± 8.06

\*Node numbers preceded by a and b correspond to Fig. 1a and b, respectively, with lineage names given where applicable.

†Fossil ages (see Supplementary Information) were applied as minimum constraints except at fixed calibration points a01, b01 and b10 (minimum constraint applied to b10 for relaxed analyses).

‡Molecular age estimates are based on penalized likelihood analyses of bayesian consensus trees (Fig. 1a and b).

§Means and standard deviations are based on penalized likelihood analyses of 1,000 randomly sampled bayesian trees; 1,000 age estimates approximated a normal distribution unless indicated.

|| Estimated ages for multiple trees were equal to the minimum age constraint.

¶ Estimated ages showed a bimodal distribution.

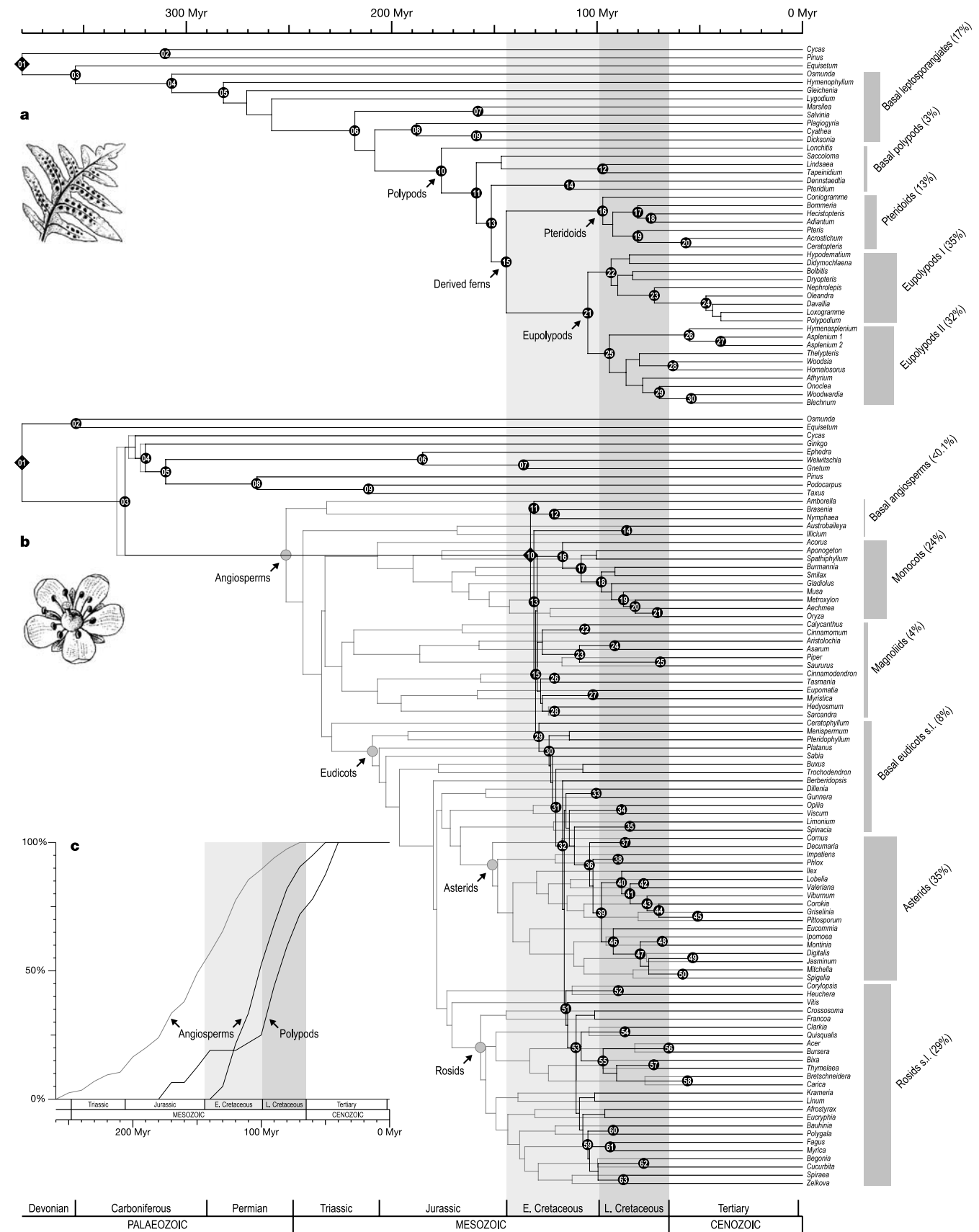


**Figure 1** Phylogenetic chronograms of ferns (**a**) and angiosperms (**b**), and proportional lineages-through-time (LTT) plots for angiosperms and polypods (**c**). For angiosperms, the black tree shows strict application of crown group fossil age at b10; grey tree shows relaxed application of this age. Numbered nodes have posterior probabilities  $\geq 0.95$ ; see Table 1 for lineage names, molecular age estimates and fossil constraints corresponding

to nodes. Nodes in the black angiosperm tree apply also to the grey tree (a few landmarks indicated: b10, b30, b36, b53). Grey boxes on right show per cent species diversity contributed by each lineage. LTT plots for angiosperms (line colour = tree colour) and polypods show number of lineages present (as a proportion of terminals) at sequential time points.

require further exploration to determine their roles in, and possible effects on, the evolution of Cretaceous terrestrial ecosystems. □

**Methods**

**Taxon sampling and DNA sequencing**

We assembled two independent data sets (ferns and angiosperms) and used the lycophyte *Huperzia* as the outgroup (not shown in Fig. 1) for both. For ferns, we sampled the chloroplast *rbcl* and *rps4* genes for 45 taxa: 41 leptosporangiate ferns from all major lineages (focusing within the polypods), one horsetail, two seed plants, and the outgroup. For angiosperms, we sampled the chloroplast *rbcl*, *atpB* and nuclear small-subunit ribosomal DNA genes for 95 taxa (mostly a subset from data set in ref. 14): 84 angiosperms, eight gymnosperms, one leptosporangiate fern, one horsetail, and the outgroup. Most DNA sequence data were already available in GenBank; 19 new fern sequences were generated as part of this study following the DNA extraction, amplification and sequencing protocols in ref. 18, and are deposited in GenBank. For fern voucher information and GenBank accession numbers see Supplementary Information.

**Phylogenetic analyses**

Phylogenetic analyses using a bayesian approach were conducted separately for ferns and angiosperms with MrBayes version 3.0b4 (ref. 29). Each gene in each data set was assigned its own model of evolution (GTR + I +  $\Gamma$  for each gene, determined using a hierarchical likelihood ratio test approach) and analyses were conducted using four chains, run for a total of 10,000,000 generations, with trees sampled from the cold chain every 1,000 generations. The resulting 10,000 trees were plotted against their likelihoods to determine the point where the likelihoods converged on a maximum value, and all 500 trees (500,000 generations) before this convergence were discarded as the 'burn-in' phase. For each data set (ferns and angiosperms), we computed a majority-rule consensus of the remaining 9,500 trees. We used this phylogenetic hypothesis (with average branch lengths), as well as 1,000 trees randomly sampled from among the 9,500 trees, in the subsequent analyses.

**Divergence time estimates**

Divergence time estimates were obtained through penalized likelihood analyses (truncated Newton algorithm) of the fern and angiosperm consensus phylogenies in r8s version 1.60 (ref. 30). For each data set, fossil age constraints were applied as indicated in Table 1 (for details see Supplementary Information) and the appropriate smoothing value was determined using cross-validation. For angiosperms, fossil age constraints<sup>22</sup> (Table 1) were applied in two ways, differing only in the application of the fossil age of the angiosperm crown group (node b10 in Fig. 1b). The first approach was strict (age fixed at 132 Myr; ref. 22) and the second relaxed (minimum age constraint of 132 Myr applied). To evaluate the effects of phylogenetic uncertainty<sup>21</sup> due to both topological and branch-length estimation error, divergence times were also estimated using penalized likelihood for each of the 1,000 randomly sampled bayesian trees for each data set. Fossil age constraints were applied as described above and individual smoothing values were determined for each tree using cross-validation. The molecular age estimates for each well-supported node (posterior probability  $\geq 0.95$ ; therefore, 950–1,000 estimates for each node, depending on support) were averaged and the standard deviation calculated.

**Lineages-through-time plots**

The chronograms resulting from the penalized likelihood analyses of the consensus phylogenies were used to calculate proportional lineages-through-time plots for polypods and angiosperms. Numbers of lineages were tallied at sequential time points (10 Myr intervals) and are presented as proportions (%) of the number of polypod or angiosperm terminals.

Received 5 November 2003; accepted 22 January 2004; doi:10.1038/nature02361.

1. Crane, P. R. in *The Origin of Angiosperms and Their Biological Consequences* (eds Friis, E. M., Chaloner, W. G. & Crane, P. R.) 107–144 (Cambridge Univ. Press, Cambridge, 1987).
2. Lidgard, S. & Crane, P. R. Angiosperm diversification and Cretaceous floristic trends: A comparison of palynofloras and leaf macrofloras. *Paleobiology* **16**, 77–93 (1990).
3. Crane, P. R., Friis, E. M. & Pedersen, K. R. The origin and early diversification of angiosperms. *Nature* **374**, 27–33 (1995).
4. Lupia, R., Lidgard, S. & Crane, P. R. Comparing palynological abundance and diversity: Implications for biotic replacement during the Cretaceous angiosperm radiation. *Paleobiology* **25**, 305–340 (1999).
5. Nagalingum, N. S., Drinnan, A. N., Lupia, R. & McLoughlin, S. Fern spore diversity and abundance in Australia during the Cretaceous. *Rev. Palaeobot. Palynol.* **119**, 69–92 (2002).
6. Niklas, K. J., Tiffney, B. H. & Knoll, A. H. Patterns in vascular land plant diversification. *Nature* **303**, 614–616 (1983).
7. Smith, A. R. Comparison of fern and flowering plant distributions with some evolutionary interpretations for ferns. *Biotropica* **4**, 4–9 (1972).
8. Lovis, J. D. Evolutionary patterns and processes in ferns. *Adv. Bot. Res.* **4**, 229–415 (1977).
9. Rothwell, G. W. in *Pteridology in Perspective* (eds Camus, J. M., Gibby, M. & Johns, R. J.) 395–404 (Royal Botanic Gardens, Kew, 1996).
10. Collinson, M. E. in *Pteridology in Perspective* (eds Camus, J. M., Gibby, M. & Johns, R. J.) 349–394 (Royal Botanic Gardens, Kew, 1996).
11. Schneider, H. & Kenrick, P. An Early Cretaceous root-climbing epiphyte (Lindsaeaceae) and its significance for calibrating the diversification of polypodiaceae ferns. *Rev. Palaeobot. Palynol.* **115**, 33–41 (2001).
12. Dilcher, D. L. Paleobotany: Some aspects of non-flowering and flowering plant evolution. *Taxon* **50**, 697–711 (2001).

13. Friis, E. M., Pederson, K. R. & Crane, P. R. Fossil evidence of water lilies (Nymphaeales) in the Early Cretaceous. *Nature* **410**, 357–360 (2001).
14. Soltis, D. E. et al. Angiosperm phylogeny inferred from 18S rDNA, *rbcl*, and *atpB* sequences. *J. Limn. Soc. Bot.* **133**, 381–461 (2000).
15. Soltis, P. S., Soltis, D. E. & Chase, M. W. Angiosperm phylogeny inferred from multiple genes as a tool for comparative biology. *Nature* **402**, 402–404 (1999).
16. Qiu, Y.-L. et al. The earliest angiosperms: Evidence from mitochondrial, plastid and nuclear genomes. *Nature* **402**, 404–407 (1999).
17. Skog, J. E. Biogeography of Mesozoic leptosporangiate ferns related to extant ferns. *Brittonia* **53**, 236–269 (2001).
18. Pryer, K. M. et al. Horsetails and ferns are a monophyletic group and the closest living relatives to seed plants. *Nature* **409**, 618–622 (2001).
19. Deng, S. Ecology of the Early Cretaceous ferns of Northeast China. *Rev. Palaeobot. Palynol.* **119**, 93–112 (2002).
20. Sanderson, M. J. Estimating absolute rates of molecular evolution and divergence times: A penalized likelihood approach. *Mol. Biol. Evol.* **19**, 101–109 (2002).
21. Pagel, M. & Lutzoni, F. in *Biological Evolution and Statistical Physics* (eds Lässig, M. & Valleriani, A.) 148–161 (Springer, Berlin, 2002).
22. Magallón, S. & Sanderson, M. J. Absolute diversification rates in angiosperm clades. *Evolution* **55**, 1762–1780 (2001).
23. Wikström, N., Savolainen, V. & Chase, M. W. Evolution of the angiosperms: Calibrating the family tree. *Proc. R. Soc. Lond. B* **268**, 2211–2220 (2001).
24. Benton, M. J. & Ayala, F. J. Dating the Tree of Life. *Science* **300**, 1698–1700 (2003).
25. Soltis, P. S., Soltis, D. E., Savolainen, V., Crane, P. R. & Barraclough, T. G. Rate heterogeneity among lineages of tracheophytes: Integration of molecular and fossil data and evidence for molecular living fossils. *Proc. Natl Acad. Sci. USA* **99**, 4430–4435 (2002).
26. Wikström, N. & Kenrick, P. Evolution of Lycopodiaceae (Lycopodiaceae): Estimating divergence times from *rbcl* gene sequences by use of nonparametric rate smoothing. *Mol. Phylogenet. Evol.* **19**, 177–186 (2001).
27. Kawai, H. et al. Responses of ferns to red light are mediated by an unconventional photoreceptor. *Nature* **421**, 287–290 (2003).
28. Smith, H. Phytochromes and light signal perception by plants—an emerging synthesis. *Nature* **407**, 585–591 (2000).
29. Huelsenbeck, J. P. & Ronquist, F. MRBAYES: Bayesian inference of phylogenetic trees. *Bioinformatics* **17**, 754–755 (2001).
30. Sanderson, M. J. r8s: Inferring absolute rates of molecular evolution and divergence times in the absence of a molecular clock. *Bioinformatics* **19**, 301–302 (2003).

Supplementary Information accompanies the paper on [www.nature.com/nature](http://www.nature.com/nature).

**Acknowledgements** We thank the Duke Biology systematics discussion group, especially P. Manos, for suggestions; F. Lutzoni, N. Nagalingum and A. R. Smith for comments on the manuscript; and M. Skakuj for the thumbnail sketches included in Fig. 1. This work was supported in part by grants from the National Science Foundation to H.S., K.M.P., R.C. and R.L.; by the Deep Time Research Coordination Network (NSF); and by the A.W. Mellon Foundation Fund to Duke University for Plant Systematics.

**Competing interests statement** The authors declare that they have no competing financial interests.

**Correspondence** and requests for materials should be addressed to K.M.P. (pryer@duke.edu). Nucleotide sequences newly determined here have been deposited in GenBank under the accession numbers AY459153–AY459171.

.....  
**Adaptation to natural facial categories**

**Michael A. Webster, Daniel Kaping, Yoko Mizokami & Paul Duhamel**

*Department of Psychology, University of Nevada, Reno, Nevada 89557, USA*

.....  
**Face perception is fundamentally important for judging the characteristics of individuals, such as identification of their gender, age, ethnicity or expression. We asked how the perception of these characteristics is influenced by the set of faces that observers are exposed to. Previous studies have shown that the appearance of a face can be biased strongly after viewing an altered image of the face, and have suggested that these after-effects reflect response changes in the neural mechanisms underlying object or face perception<sup>1–5</sup>. Here we show that these adaptation effects are pronounced for natural variations in faces and for natural categorical judgements about faces. This**